Journal of Magnetic Resonance **148,** 61–72 (2001)
doi:10.1006/jmre.2000.2222, available online at http://www.idealibrary.com on IDEAL®

MUSIC, Selective Pulses, and Tuned Delays: Amino Acid Type-Selective $^{1}H–^{15}N$ Correlations, II

Mario Schubert, Hartmut Oschkinat, and Peter Schmieder[1]

Forschungsinstitut für Molekulare Pharmakologie, Robert-Roessle-Str. 10, D-13125 Berlin, Germany

Received May 22, 2000; revised August 21, 2000

Amino acid type-selective experiments help to remove ambiguities in either manual or automated assignment procedures. Here we present modified triple-resonance experiments that yield amino acid type-selective $^{1}H–^{15}N$ correlations. They are based on the MUSIC coherence transfer scheme which replaces the initial INEPT transfer and is selective for XH_2 or XH_3 (where X is either ^{15}N or ^{13}C). Signals of the desired amino acid types are thus selected based on the topology of the side chain. MUSIC is combined with selective pulses and carefully tuned delays to create experiments for Ser (S–HSQC); Val, Ile, and Ala (VIA–HSQC); Leu and Ala (LA–HSQC); Asp, Asn, and Gly (DNG–HSQC), as well as Glu, Gln, and Gly (EQG–HSQC). The new experiments are recorded as two-dimensional spectra and their performance is demonstrated by their application to two protein domains of 83 and 115 residues.

Key Words: **triple-resonance; proteins; editing; HSQC; assignment; MUSIC.**

INTRODUCTION

In the past decade triple-resonance experiments (*1, 2*) have been routinely used for the assignment of protein spectra. This is mainly due to their high sensitivity, their intrinsically good resolution, and their independence from the three-dimensional structure of the molecule under investigation. Moreover, the ease of interpretation makes these spectra ideally suited for automated or semi-automated assignment procedures (*3–7*). Many variations and extensions of the original triple-resonance schemes have been presented (*8–14*), among them amino acid type-selective experiments (*15–36*) that yield specific information which is helpful in manual or automated assignment procedures. Most assignment protocols use a ^{15}N–HSQC spectrum as a starting point and correlate the (^{1}H,^{15}N) frequency pairs with carbon or proton frequencies in a third dimension to achieve a sequence-specific assignment.

We have recently presented a set of 12 amino acid type-selective ^{1}H,^{15}N correlations (*37*) that were designed to support this assignment strategy. These experiments are based on the MUSIC (multiplicity selective in-phase coherence transfer) pulse sequence building block (*38, 39*), which accomplishes a coherence transfer to or from the heteronucleus, selective for XH_2 or XH_3 (where X is either ^{15}N or ^{13}C). It selects multiplicity via multiple-quantum filters and offers superior suppression of unwanted signals compared to sequences which work solely by the appropriate tuning of delays to select for the number of coupling partners or the use of selective pulses. When MUSIC is implemented in the appropriate triple-resonance experiment, the signals of the desired amino acid types are selected based on the topology of the side chain. MUSIC does not lengthen the sequence compared to the standard triple-resonance experiments, therefore no loss of intensity occurs due to relaxation.

Here we extend the set of these pulse sequences by another 10 amino acid type-selective ^{1}H,^{15}N correlations based on the same principle, selective for Ser (S–HSQC); Val, Ile, and Ala (VIA–HSQC); Leu and Ala (LA–HSQC); Asp, Asn, and Gly (DNG–HSQC), as well as Glu, Gln, and Gly (EQG–HSQC). As in the previous set, 5 of the 10 experiments represent the (i + 1) version and the other 5 the (i, i + 1) version of an amino acid type-selective $^{1}H–^{15}N$ correlation. The latter experiments are somewhat less sensitive and can potentially contain two signals per residue, of which the (i + 1) will usually be weaker. Coherence selection with the MUSIC step is now combined with the use of selective pulses. Thus the chemical shifts of the carbon atoms in the side chain are used as additional criteria for the selection of an amino acid. The resulting spectra exhibit the clean selection of the MUSIC step enhanced by exploiting the high degree of dispersion of the side chain carbon resonances. They are applied to two different protein domains, the SAM domain from EphB2 (*40, 41*) and the EVH1 domain from VASP (*42, 43*), the structures of which have been determined using NMR spectroscopy. The first is a small, α-helical domain of 83 residues and the second a larger, 115-residue domain with a high β-sheet content.

RESULTS

To create the new experiments, the MUSIC step was implemented in standard triple-resonance pulse sequences. The magnetization transfer pathways selected by the resulting pulse

[1] To whom correspondence should be addressed. Fax: +49-30-94793-230. E-mail: schmieder@fmp-berlin.de.

1090-7807/01 $35.00

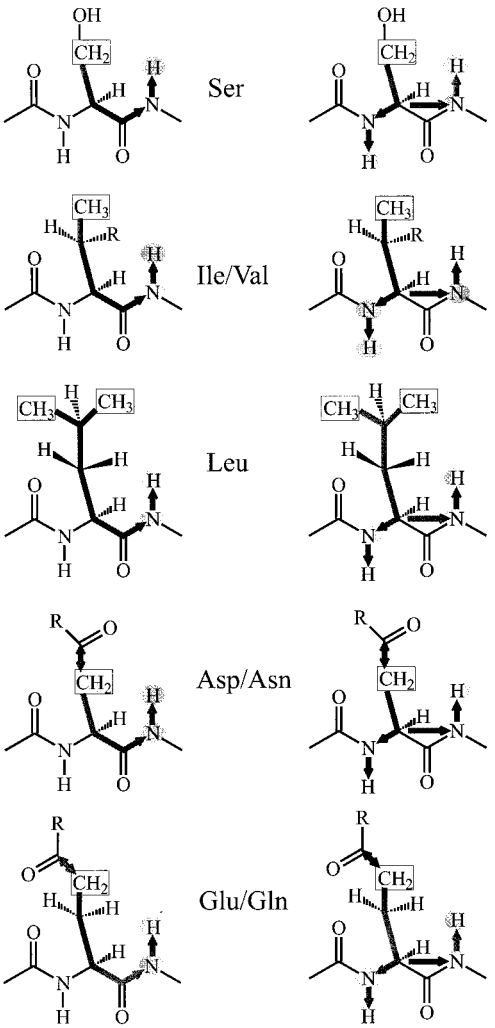

FIG. 1. Schematic representation of the magnetization pathway selected by the new experiments. First a particular group (CH_2 or CH_3, indicated by the hatched rectangle) is selected with the MUSIC sequence. From there the magnetization is transferred along the side chain to the C^α carbon and finally to the amide proton, as indicated by the arrows. The two types of pulse sequences differ in the transfer from the C^α to the nitrogen. In the left column the flow of magnetization in the $(i + 1)$-HSQCs is depicted, from the C^α to the carbonyl and then to the nitrogen and amide proton. The right column represents the $(i, i + 1)$-HSQCs, where the magnetization flows from the C^α to either the nitrogen of the same amino acid or that of the $(i + 1)$ neighbor. In the case of Asp/Asn and Glu/Gln a HMQC-type filter for the side chain carbonyls is implemented at the beginning.

sequences are depicted in Fig. 1. At the beginning of the sequence a particular group (CH_2 or CH_3) is selected with MUSIC. Subsequently, the magnetization is transferred along the side chain to the C^α. From the C^α, the magnetization is relayed either via the carbonyl carbon to the $(i + 1)$ nitrogen or directly to both nitrogens coupled to the C^α (i or $i + 1$). Finally, the amide proton signal is detected. During the transfer, signal selection is enhanced by selective pulses and appropriately tuned delays. Both help to discriminate between amino acid side chains that exhibit a similar topology but differ in the chemical shift or the number of coupling partners of certain side chain carbons.

Ser

The implementation of a MUSIC–CH_2 selection into the beginning of the CBCA(CO)NNH (*44*) or CBCANNH (*45*) experiment would select all amino acids with a methylene group as C^β (all except Thr, Ile, and Val) and Gly. Serine, however, is the only one of those amino acids that has a C^β with a unique chemical shift between 60 and 70 ppm (*46*). This fact can be exploited by the use of selective pulses to create serine-selective experiments. The pulse sequences are shown in Figs. 2a and 2b. Both carbon 180° pulses in the beginning of the sequence are replaced by REBURP pulses (*47*) with a length of 2048 μs centered at 60.5 ppm. They cover a range of 18 ppm and affect both the serine C^α and the C^β. The C^β magnetization of the other amino acids selected by MUSIC is, however, unperturbed by the REBURP pulses while the C^α is inverted. Since no coupling between C^β and C^α will thus evolve, no magnetization can be transferred to the C^α and hence to the NH. The Gly C^α magnetization is also unperturbed by the REBURP pulses. This prevents the evolution of coupling between the C^α and the C' in the $(i + 1)$ version of the experiment and hence the magnetization transfer to the NH. The same is true for the $(i, i + 1)$ version of the experiment, where the evolution of coupling between the C^α and the N is prevented. The resulting two-dimensional spectra are shown in Figs. 3a and 3b.

Asp, Asn, Gly (DNG)

The C^β of Asp and Asn, the C^γ of Glu and Gln, and the C^α of Gly are the only CH_2 groups that show a coupling to an adjacent carbonyl carbon. This fact can be used to create further amino acid type-selective experiments. The MUSIC–CH_2 selection is therefore combined with an HMQC type sequence (*48, 49*) and both are implemented in the CBCA-(CO)NNH (*44*) and the CBCANNH (*45*) experiment. The resulting pulse sequences are shown in Figs. 2c and 2d. The flow of magnetization is best described using product operators: During Δ_1 antiphase magnetization $2C_y^\beta C_z'$ is created (point a). A selective 90° pulse affecting only the carbonyl region converts it into multiple-quantum coherence $2C_y^\beta C_y'$ which is selected by alternating the phase of the consecutive, selective 90° carbonyl pulse. This pulse converts the multiple-quantum coherence back to $2C_y^\beta C_z'$ magnetization which is refocused during the second Δ_1 delay. Self-refocusing L0S2-0 pulses (*50, 51*) with a duration of 512 μs (covering a range of 72 ppm) centered at 185 ppm were used. During $2\Delta_1$ the coupling between C^β and C^α can evolve and antiphase magnetization $2C_y^\beta C_z^\alpha$ is created (point b). The next 90° carbon pulse converts it into $2C_z^\beta C_y^\alpha$ which is refocused during $2\Delta_3$ (or $2\Delta_4$). The magnetization is then transferred from the C^α to the

amide proton. The resulting transfer functions for the experiments in Figs. 2c and 2d are

$$\sin^2(\pi J_{CCO}\Delta_1)\sin(\pi J_{CC}2\Delta_1)\sin(\pi J_{CC}2\Delta_3)\sin(\pi J_{CC'}2\Delta_3) \quad [1]$$

$$\sin^2(\pi J_{CCO}\Delta_1)\sin(\pi J_{CC}2\Delta_1)\sin(\pi J_{CC}2\Delta_4)\sin(\pi J_{CN}2\Delta_4). \quad [2]$$

Neglecting relaxation effects, the nominal values for Δ_1, Δ_3, and Δ_4 are 8.2, 5.3, and 9 ms, respectively. An experimental optimization resulted in a value of 4.5 ms for Δ_3. Since there is only one COSY transfer step, magnetization from the C^γ of Glu and Gln cannot be transferred to the amino proton and is suppressed. Magnetization from the C^α of Gly is not affected by the 90° pulse after point b. Coupling between the C^α and C' (or N) will evolve during $2\Delta_3$ (or $2\Delta_4$) and magnetization is transferred to the amide proton. The resulting spectra will thus contain signals originating from Asp, Asn, and Gly and are shown in Figs. 4a and 4b.

Glu, Gln, Gly (EQG)

An extension of the DNG pulse sequences by an additional COSY step on carbon leads to a selection of Glu and Gln in addition to Asp, Asn, and Gly (Figs. 2c and 2d).

In analogy to the DNG experiments, antiphase magnetization $2C_y^\gamma C_z'$ is created, selected, and refocused during $2\Delta_1$, while coupling between the C^γ and C^β is active and antiphase magnetization $2C_y^\gamma C_z^\beta$ is created (point b). It is converted into $2C_z^\gamma C_y^\beta$ by the next 90° carbon pulse. During $2\Delta_2$ antiphase magnetization $2C_z^\gamma C_y^\beta$ is refocused and coupling to C^α leads to antiphase magnetization $2C_y^\beta C_z^\alpha$ (point c). The next 90° carbon

FIG. 2. Pulse sequences of the new amino acid type-selective ^1H–^{15}N correlations. The pulse sequences yield spectra for Ser (a and b), Asp/Asn/Gly or Glu/Gln/Gly (c and d), and Ile/Val/Ala or Leu/Ala (e and f). The 90 and 180° pulses are represented by thin black filled and thick unfilled bars, respectively. The water-selective 90° ^1H flip-back pulse is represented by a striped thick bar; a hatched thin bar stands for a 90° flip-back ^1H pulse at the end of the ^1H-decoupling sequence. Magnetic field gradients as well as shaped 180° ^{13}CO pulses are represented by sine shapes. Pulses applied at the $^{13}C^{\alpha/\beta}$ or ^{13}CO resonance frequencies were adjusted to provide a null at the corresponding ^{13}CO or $^{13}C^\alpha$ frequencies. The square $^{13}C^{\alpha/\beta}$ 90° and 180° pulses were set to 49 and 44 μs, respectively. The square ^{13}CO 90° and 180° pulses were set to 54 and 108 μs, respectively. The shaped 180° ^{13}CO were applied as a G3 Gaussian cascade (*54*) with a duration of 256 μs. The striped thick bars stands for band-selective 180° REBURP pulses (*47*). The offsets and pulse lengths are given in the description of the particular experiments. Self-refocusing selective L0S2-0 excitation pulses (*50, 51*) with a duration of 512 μs at 185 ppm are represented by filled sine shapes. The second L0S2-0 pulse has a time-inverted shape. Unless indicated otherwise, pulses are applied with phase x. Proton hard pulses were applied with 25-kHz field strength; WALTZ-16 (*55*) of ^1H spins was achieved using a field strength of 3.1 kHz. The same field strength was used for the subsequent 90° flip-back ^1H pulse. The water-selective 90° square pulse had a duration of 1 ms. GARP-1 decoupling (*56*) of ^{15}N was achieved using a field strength of 830 Hz. Water suppression was obtained using WATERGATE implemented with a 3–9–19 pulse (*57*). The gradients were applied as a sinusoidal function from 0 to π. The carrier frequencies were centered at ^1H = 4.8 ppm, ^{15}N = 119.6 ppm, $^{13}C^{\alpha/\beta}$ = 45 ppm, and ^{13}CO = 175 ppm. The following delays were used: τ_1 = 3.5 ms, τ_1' = 4 ms, τ_2 = 5.5 ms, τ_3 = 2.25 ms, δ_0 = 4.5 ms, δ_1 = 6.9 ms, δ_2 = 11.4 ms, δ_3 = 9 ms, T_N = 11 ms, T_R = 4 ms (7.1 ms for the LA–HSQCs), T_R' = 3.6 ms, T_C = 4.5 ms, Δ_1 = 8 ms (9 ms for the EQG-(i + 1)–HSQC, 7.1 ms for the EQG-(i, i + 1)–HSQC), Δ_2 = 4.5 ms, Δ_3 = 4.5 ms, and Δ_4 = 9 ms (7.1 ms for the EQG-(i, i + 1)–HSQC). To achieve quadrature detection in the indirect dimension the States–TPPI–States protocol (*58*) was used in all experiments. All spectra were processed using XWINNMR (Bruker AG). (a) S-(i + 1)–HSQC. The phase cycling was: ϕ_1 = 16 (x), 16 ($-x$); ϕ_2 = 2 (45°), 2 (135°), 2 (225°), 2 (315°); ϕ_3 = x, $-x$; ϕ_4 = 50°; ϕ_5 = x; ϕ_6 = 8 (x), 8 (y), 8 ($-x$), 8 ($-y$); ϕ_7 = 4 ($-y$), 4 (y); ϕ_8 = $-x$; ϕ_{rec} = 2 (x, 2 ($-x$), x), 4 ($-x$, 2 x, $-x$), 2 (x, 2 ($-x$), x). States–TPPI phase cycling was applied to ϕ_5. Gradients had the following duration and strength: G_1 = 800 μs (7 G/cm), G_2 = 800 μs (28 G/cm), G_3 = 1 ms (21 G/cm). Two selective REBURB pulses with a duration of 2048 μs at 60.5 ppm were used. (b) S-(i, i + 1)–HSQC. The phase cycling was: ϕ_1 = 16 (x), 16 ($-x$); ϕ_2 = 2 (45°), 2 (135°), 2 (225°), 2 (315°); ϕ_3 = x, $-x$; ϕ_4 = 8 (x), 8 (y), 8 ($-x$), 8 ($-y$); ϕ_5 = 4 ($-y$), 4 (y); ϕ_6 = ($-x$); ϕ_{rec} = 2 (x, 2 ($-x$), x), 4 ($-x$, 2 x, $-x$), 2 (x, 2 ($-x$), x). States–TPPI phase cycling was applied to phase ϕ_3. The gradients had the following duration and strength: G_1 = 800 μs (7 G/cm), G_2 = 800 μs (28 G/cm), G_3 = 1 ms (21 G/cm). Two selective REBURB pulses with a duration of 2048 μs at 60.5 ppm were used. (c) DNG-(i + 1)–HSQC (omitting the part in the parenthesis) and EQG-(i + 1)–HSQC (including the part in the parenthesis). The phase cycling was as follows: ϕ_1 = 16 (x), 16 ($-x$); ϕ_2 = 2 (45°), 2 (135°), 2 (225°), 2 (315°); ϕ_3 = x, $-x$, ϕ_4 = 50°; ϕ_5 = x, ϕ_6 = 8 (x), 8 (y), 8 ($-x$), 8 ($-y$); ϕ_7 = 4 ($-y$), 4 (y); ϕ_8 = $-x$; ϕ_{rec} = 2 (x, 2 ($-x$), x), 4 ($-x$, 2 (x), $-x$), 2 (x, 2 ($-x$), x). States–TPPI phase cycling was applied to phase ϕ_5. The gradients had the following duration and strength: G_1 = 1 ms (7 G/cm), G_2 = 800 μs (28 G/cm), G_3 = 1 ms (21 G/cm). (d) DNG-(i, i + 1)–HSQC (omitting the part in the parenthesis) and EQG-(i, i + 1)–HSQC (including the part in the parenthesis). The phase cycling was: ϕ_1 = 16 (x), 16 ($-x$); ϕ_2 = 2 (45°), 2 (135°), 2 (225°), 2 (315°); ϕ_3 = x, $-x$; ϕ_4 = 32 (x), 32 ($-x$); ϕ_5 = 8 (x), 8 (y), 8 ($-x$), 8 ($-y$); ϕ_6 = 4 ($-y$), 4 (y); ϕ_7 = $-x$; ϕ_{rec} = 2 (x, 2 ($-x$), x), 4 ($-x$, 2 (x), $-x$), 2 (x, 2 ($-x$), x), 2 ($-x$, 2 (x), $-x$), 4 (x, 2 ($-x$), x), 2 ($-x$, 2 (x), $-x$). States–TPPI phase cycling was applied to phase ϕ_4. The gradients had the following duration and strength: G_1 = 1 ms (7 G/cm), G_2 = 800 μs (28 G/cm), G_3 = 1 ms (21 G/cm). (e) VIA-(i + 1)–HSQC (omitting the part in the parenthesis), LA-(i + 1)–HSQC (including the part in the parenthesis). The phase cycling was: ϕ_1 = 24 (x), 24 ($-x$); ϕ_2 = 2 (30°), 2 (90°), 2 (150°), 2 (210°), 2 (270°), 2 (330°); ϕ_3 = x, $-x$; ϕ_4 = 50°; ϕ_5 = x; ϕ_6 = 12 (x), 12 (y), 12 ($-x$), 12 ($-y$); ϕ_7 = $-y$; ϕ_8 = $-x$; ϕ_{rec} = 3 (x, 2 ($-x$), x), 6 ($-x$, 2 (x), $-x$), 3 (x, 2 ($-x$), x). States–TPPI phase cycling was applied to phase ϕ_5. The gradients had the following duration and strength: G_1 = 800 μs (7 G/cm), G_2 = 800 μs (28 G/cm), G_3 = 1 ms (21 G/cm). In the VIA-(i + 1)–HSQC the pulse S_1 is a selective REBURB pulse with a duration of 768 μs at 26.7 ppm; S_3 is a rectangular pulse with a duration of 44 μs. In the LA-(i + 1)–HSQC three REBURB pulses are applied: S_1 = 1024 μs at 18.5 ppm, S_2 = 768 μs at 35 ppm, S_3 = 1024 μs at 48 ppm. (f) VIA-(i, i + 1)–HSQC (omitting the part in the parenthesis), VIA-(i, i + 1)–HSQC (including the part in the parenthesis). The phase cycling was: ϕ_1 = 24 (x), 24 ($-x$); ϕ_2 = 2 (30°), 2 (90°), 2 (150°), 2 (210°), 2 (270°), 2 (330°); ϕ_3 = x, $-x$; ϕ_4 = 12 (x), 12 (y), 12 ($-x$), 12 ($-y$); ϕ_5 = $-y$; ϕ_6 = $-x$; ϕ_{rec} = 3 (x, 2 ($-x$), x), 6 ($-x$, 2 (x), $-x$), 3 (x, 2 ($-x$), x). States–TPPI phase cycling was applied to phase ϕ3. The gradients had the following duration and strength: G_1 = 800 μs (7 G/cm), G_2 = 800 μs (28 G/cm), G_3 = 1 ms (21 G/cm). The same selective pulses as in the VIA-(i + 1)–HSQC and LA-(i + 1)–HSQC were used.

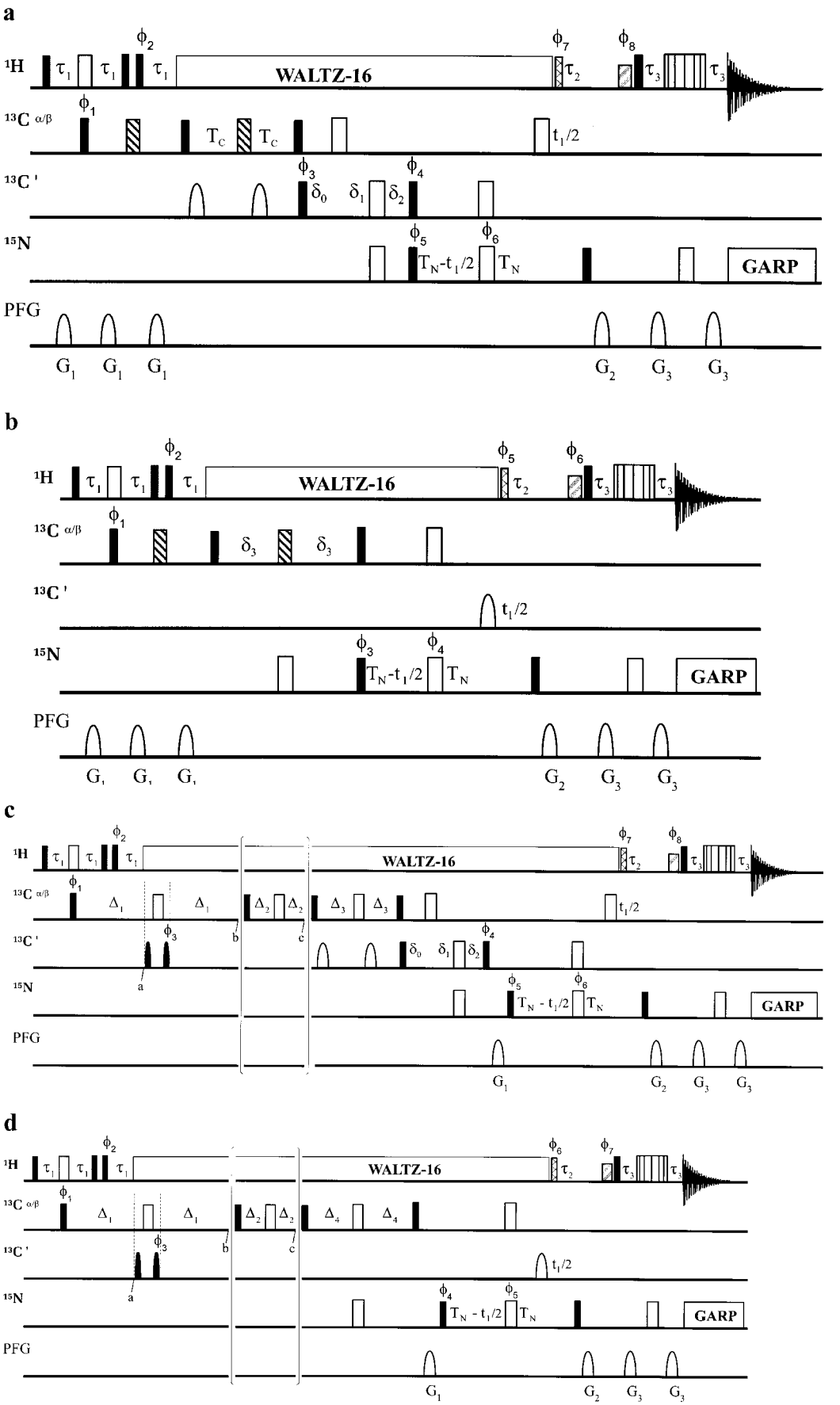
a
b
c
d
WALTZ-16
GARP
PFG

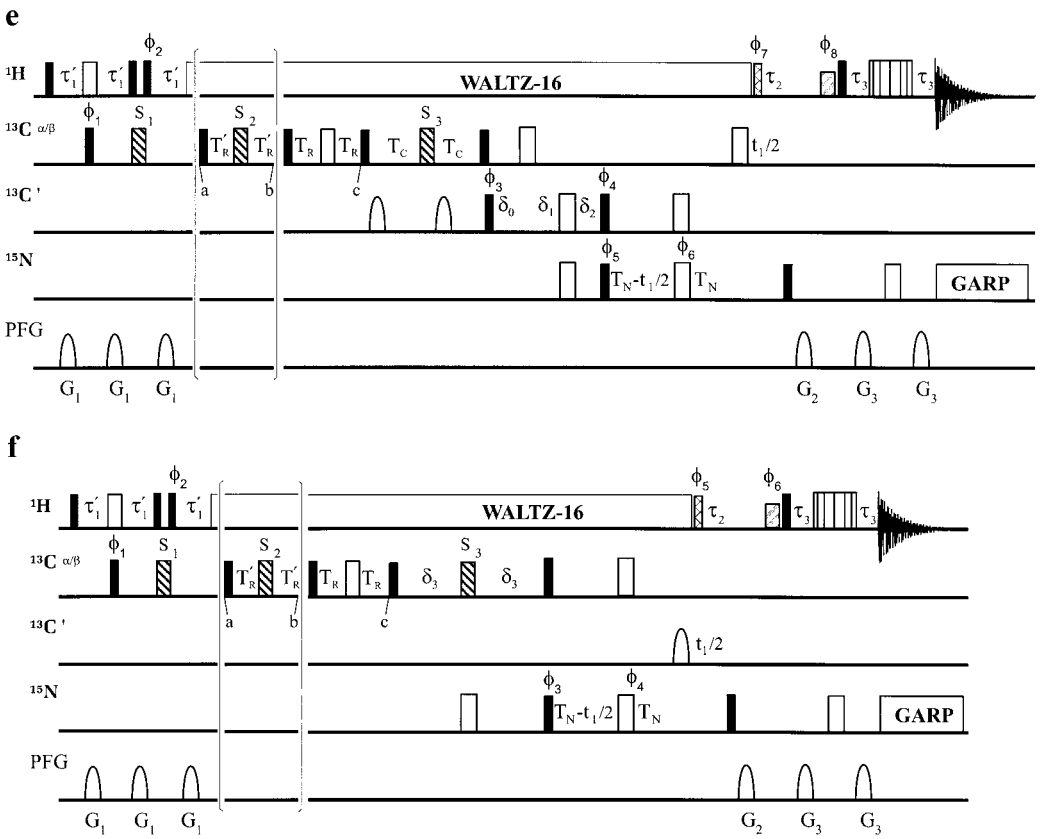

FIG. 2—*Continued*

pulse creates antiphase magnetization $2C_z^{\beta}C_y^{\alpha}$ which is refocused during $2\Delta_3$ (or $2\Delta_4$). From the C^{α} the magnetization is transferred to the amino proton in the usual manner.

The resulting transfer functions for the experiment EQG-(i + 1) in Fig. 2c is

$$\sin^2(\pi J_{CCO}\Delta_1)\sin(\pi J_{CC}2\Delta_1)\sin^2(\pi J_{CC}2\Delta_2) \times \sin(\pi J_{CC}2\Delta_3)\sin(\pi J_{CN}2\Delta_3). \quad [3]$$

In addition, there are two possible magnetization pathways for Asn and Asp in this experiment: C_x^{β} remains in-phase with respect to C^{α} during $2\Delta_1$ and is converted into C^{α} magnetization during $2\Delta_2$ and $2\Delta_3$ or C_x^{α} is already formed at the end of $2\Delta_2$ and remains in-phase with respect to the C^{β} during $2\Delta_3$. The resulting transfer functions are

$$\sin^2(\pi J_{CCO}\Delta_1)\cos(\pi J_{CC}2\Delta_1) \times \sin(\pi J_{CC}2\Delta_2)\sin(\pi J_{CC}2\Delta_3)\sin(\pi J_{CC'}2\Delta_3) \quad [4]$$

$$\sin^2(\pi J_{CCO}\Delta_1)\sin(\pi J_{CC}2\Delta_1) \times \sin(\pi J_{CC}2\Delta_2)\cos(\pi J_{CC}2\Delta_3)\sin(\pi J_{CC'}2\Delta_3). \quad [5]$$

Analyzing transfer function [3] nominal delays for Δ_1, Δ_2, and Δ_3 are 8.2, 7.1, and 5.3 ms, respectively, to obtain optimal signal to noise for Glu and Gln. With these delays the signals of Gly, Glu, and Gln have opposite sign to those of Asn and Asp. This can result in cancellation of signals if peaks from both types of amino acids overlap. To avoid this, the delays Δ_1 and Δ_3 can be tuned such that signals from Asp and Asn are suppressed. The two pathways [4] and [5] cancel if $\Delta_1 + \Delta_3 = 1/2J_{CC} = 14.2$ ms. Neglecting relaxation and the length of the two selective C′-pulses, optimal delays for Glu and Gln are then $\Delta_1 = 8.7$ ms, $\Delta 3 = 5.5$ ms. In an experimental optimization with the EVH1 domain the suppression of signals form Asp and Asn worked best with $\Delta_1 = 9$ ms, $\Delta_2 = 4.5$ ms, and $\Delta_3 = 4.5$ ms.

The transfer functions for the EQG-(i, i + 1) pulse sequence in Fig. 2d are similar to [3], [4], and [5], only Δ_3 and $J_{CC'}$ are replaced by Δ_4 and J_{CN}, leading to the nominal values for Δ_1, Δ_2, and Δ_4 of 8.2, 7.1, and 9 ms, respectively. As in the (i + 1) sequence, these delays will lead to opposite sign for signals from Gly, Glu, and Gln relative to those from Asn and Asp. Cancellation will then occur not only if peaks from both types of amino acids overlap but also if amino acids of both types are adjacent in the sequence. Using the condition $\Delta_1 + \Delta_4 = 1/2J_{CC} = 14.2$ ms for the suppression of signals from Asn and Asp, optimal delays are $\Delta_1 = 7.1$ ms, $\Delta_4 = 7.1$ ms. The result of an experimental optimization was $\Delta_1 = 7.1$ ms, $\Delta_2 = 4.5$ ms, and $\Delta_4 = 7.1$ ms.

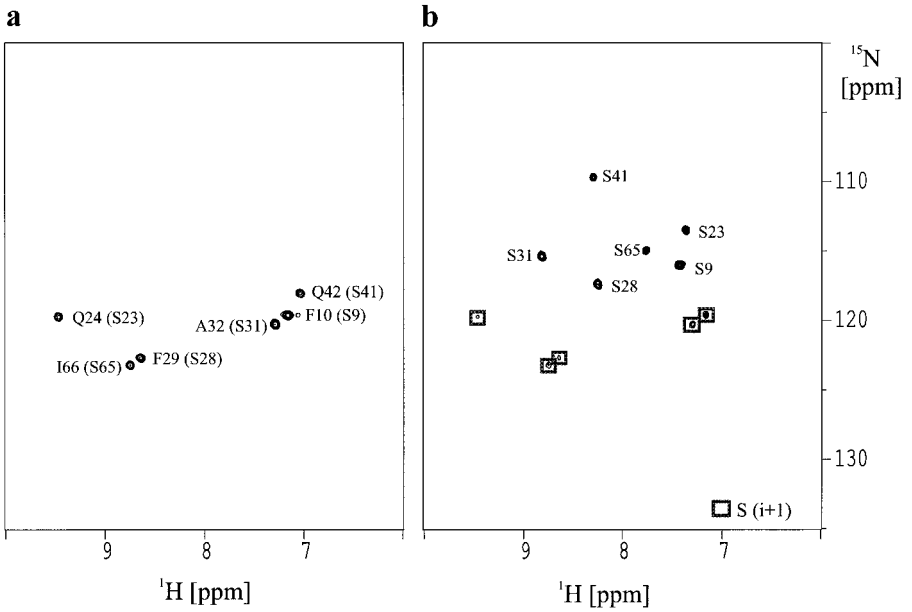

FIG. 3. Amino acid type-selective ^{1}H–^{15}N correlations of the SAM domain from EphB2. (a) The S-(i + 1)–HSQC was acquired in 1 h 30 min using 32 scans per complex point. The SAM domain contains six serines which results in six strong signals from sequential neighbors of Ser. (b) The S-(i, i + 1)–HSQC was acquired in 1 h 30 min using 32 scans per complex point. In addition to the six signals of the Ser residues five of the sequential neighbors are also present with weak intensity. They are marked with small rectangles.

Asp and Asn cannot always be totally suppressed, however, since J_{CC} can vary and some small negative signals appear in the spectra, which are shown in Figs. 4c and 4d.

Val, Ile, Ala (VIA)

The implementation of a MUSIC–CH_3 sequence in the CBCA(CO)NNH and CBCANNH sequences that have been extended by a relay step results in a selection of Val, Ile, Thr, and Ala, the TAVI–HSQC (*37*). A further selection is possible by the implementation of selective pulses into the pulse sequences, which are shown in Figs. 2e and 2f. One option is to replace the 180° pulse S_3 by a 1024-μs REBURP pulse (covering a range of 36 ppm) centered at 68.5 ppm, which results in a spectrum containing Thr and Ala (*37*). A Val/Ile/Ala (VIA) selective experiment can be obtained in a similar manner by replacing the 180° pulse S_1 by a REBURP pulse of 768 μs (covering a range of 48 ppm) which is centered at 26.7 ppm. It will affect the magnetization of the C^{γ} and C^{β} of both Val and Ile but not the C^{β} magnetization of Thr. The transfer of magnetization from C^{γ} to C^{β} in Thr and thus the transfer to the C^{α} in the next COSY step will not be effective anymore, hence Thr is suppressed. Spectra are shown in Figs. 5a and 5b.

Leu, Ala (LA)

To create an experiment which is selective for Leu, the two δ-CH_3 groups are selected with a MUSIC–CH_3 selection. Then the magnetization is transferred along the side chain to the backbone C^{α}. This could be achieved by several COSY steps or by a TOCSY transfer. We choose the first option since it offers the possibility of further differentiating between desired and undesired magnetization transfer pathways by selective pulses and by appropriate tuning of delays. The recently published TAVI experiments were used as a starting point and an additional COSY step was implemented (Figs. 2e and 2f). This allows the magnetization from Leu C^{δ} to reach the backbone NH. Without an additional selection, however, the resulting spectra (not shown) contain signals originating from Leu, Val, Ile, Thr, and Ala. A combination of selective pulses and appropriately tuned delays was used to suppress Thr, Val, and Ile and thus further simplify the spectra. Three selective REBURP pulses were implemented in the pulse sequence (S_1, S_2, and S_3 in Figs. 2c and 2d). Their excitation profile is shown in Fig. 6 together with the statistical chemical shifts of the amino acids involved (*46*). The REBURP pulse S_1 had a length of 1024 μs and was centered at 18.5 ppm. The pulse affects both the C^{δ} and the C^{γ} of Leu during $2\tau_1'$. Antiphase magnetization $2C_y^{\delta}C_z^{\gamma}$ is created and converted by a 90° pulse to $2C_z^{\delta}C_y^{\gamma}$ (point a). The second REBURP pulse S_2 at 35 ppm (with a length of 768 μs) affects the C^{δ}, C^{γ}, and C^{β} of Leu. Antiphase magnetization $2C_z^{\delta}C_y^{\gamma}$ is refocused with respect to the C^{δ} and evolves into antiphase magnetization $2C_y^{\gamma}C_z^{\beta}$ during $2T_R'$ (point b). During the same time the magnetization of interest stays in-phase with respect to the other C^{δ}. This antiphase magnetization $2C_y^{\gamma}C_z^{\beta}$ is converted to $2C_z^{\gamma}C_y^{\beta}$ and

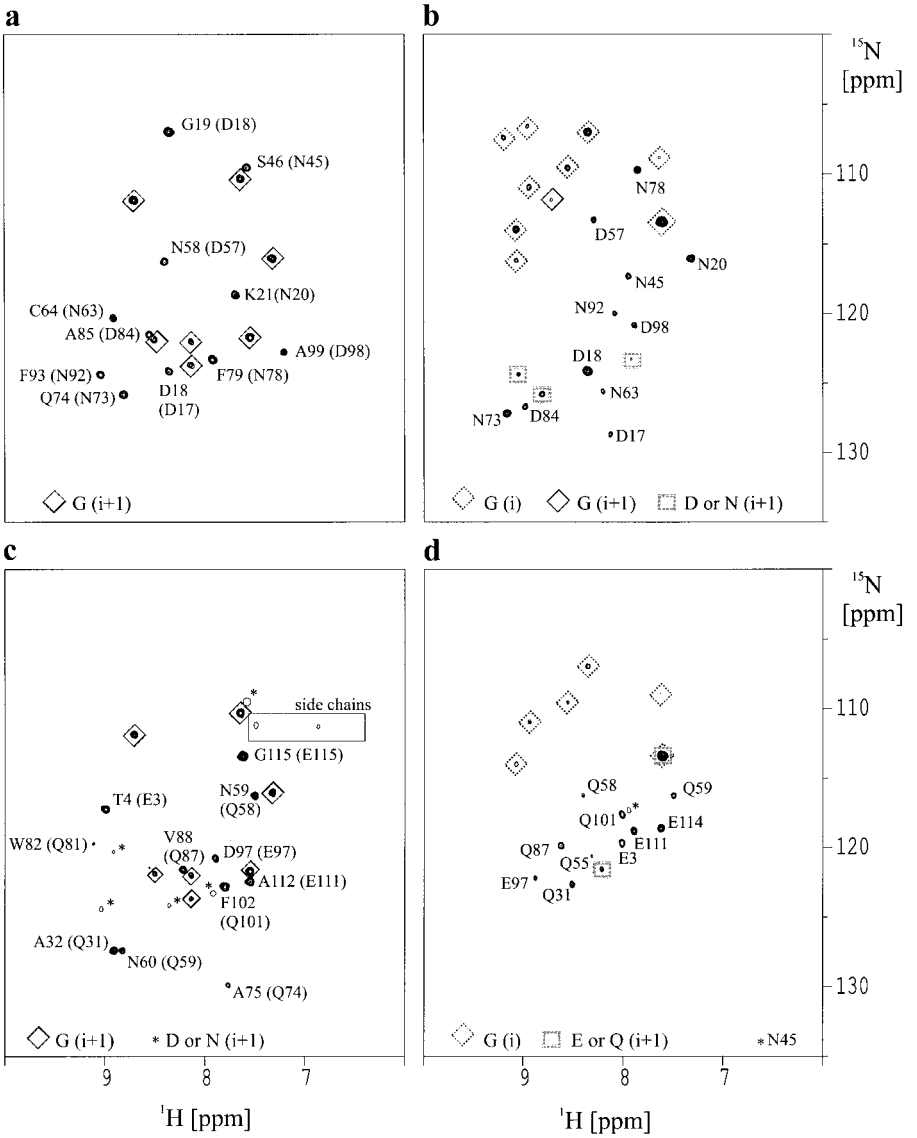

FIG. 4. Amino acid type-selective ^{1}H–^{15}N correlations of the EVH1 domain from VASP. The EVH1 domain contains 4 Glu, 9 Gln, 5 Asp, 7 Asn, and 9 Gly. (a) The DNG-(i + 1)–HSQC was acquired in 1 h 30 min using 32 scans per complex point. All expected signals (six N (i + 1), five D (i + 1)) are visible. N41 is followed by P42 and gives no signal. The glycine neighbors (marked with thin rectangles) can be identified using the G-(i + 1)–HSQC and the asparagine neighbors using the N-(i + 1)–HSQC. (b) The DNG-(i, i + 1)–HSQC was acquired in 3 h using 64 scans per complex point and contains all Asp, six of seven Asn, and all Gly residues. The (i + 1) peaks are marked with thick rectangles (c) The EQG-(i + 1)–HSQC was acquired in 3 h using 64 scans per complex point. It contains all four E-(i + 1) and seven of eight Q-(i + 1) signals. Q55 is followed by P56 and cannot give a signal. The suppression of D/N-(i + 1) peaks is achieved by appropriate tuning of $\Delta 1$ and $\Delta 4$. However, some breakthrough peaks of Asn/Asp (marked with an asterisk) and weak signals from side chain NDH groups show up. (d) The EQG-(i, i + 1)–HSQC was acquired in 4 h 30 min using 96 scans per complex point and contains all four Glu and six of nine Gln signals. Signals from Asp/Asn are suppressed except N45, which appears as a negative signal (marked with an asterisk).

refocused during $2T_R$ while coupling to the α-carbon leads to $2C_y^\beta C_z^\alpha$ (point c). This is converted into $2C_z^\beta C_y^\alpha$ and is refocused during T_c (or δ_3) because the third REBURP pulse S_3 at 48 ppm (with a length of 1024 μs) allows coupling between Leu C^α and C^β. Taken together, this results in the following transfer functions for Leu:

$$\sin(\pi J_{CC} 2\tau_1')\sin^2(\pi J_{CC} 2T_R') \times \cos(\pi J_{CC} 2T_R')\sin^2(\pi J_{CC} 2T_R)\sin(\pi J_{CC} 2T_C) \quad [6]$$

$$\sin(\pi J_{CC} 2\tau_1')\sin^2(\pi J_{CC} 2T_R') \times \cos(\pi J_{CC} 2T_R')\sin^2(\pi J_{CC} 2T_R)\sin(\pi J_{CC} 2\delta_3). \quad [7]$$

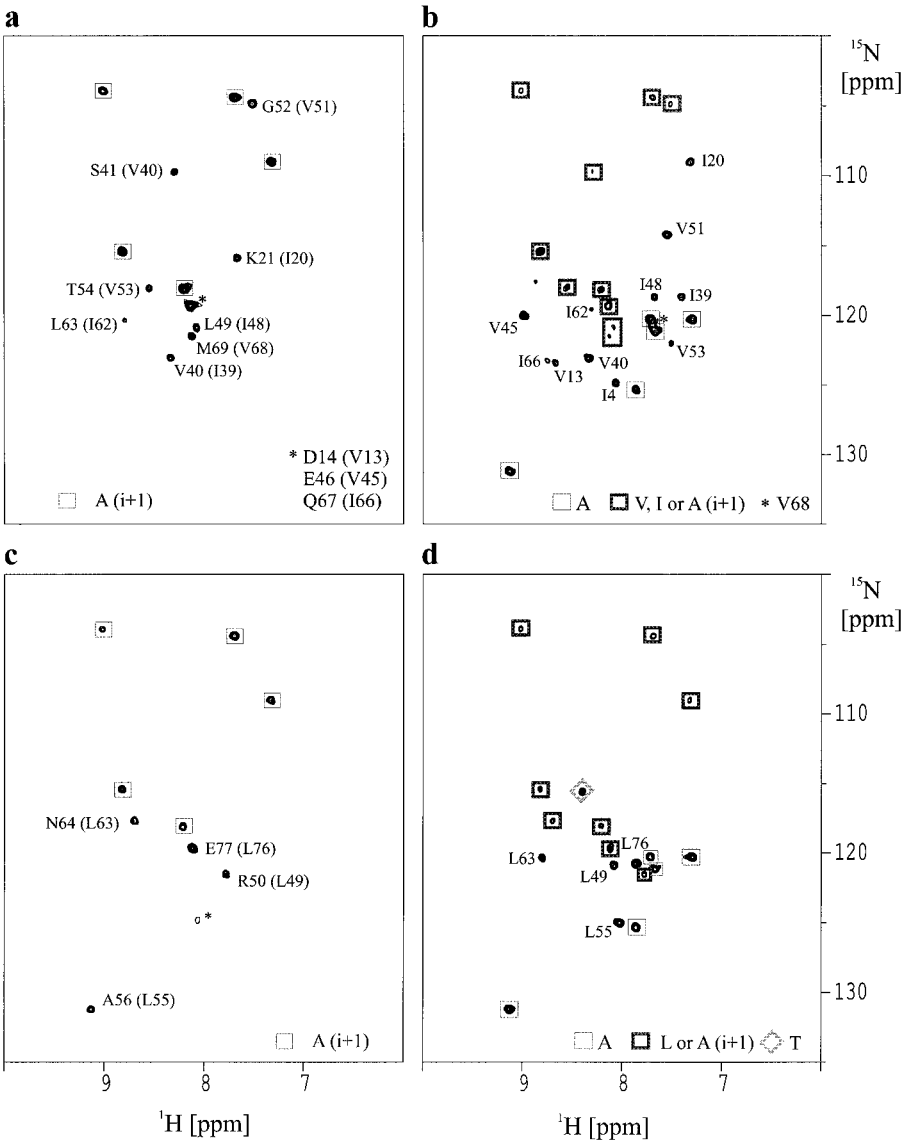

FIG. 5. Amino acid type-selective ^{1}H–^{15}N correlations of the SAM domain from EphB2. (a) The VIA-(i + 1)–HSQC was acquired in 2 h 15 min using 48 scans per complex point. (b) The VIA(i, i + 1)–HSQC was acquired in 4 h 30 min using 96 scans per complex point. The SAM domain contains 7 threonines, 6 isoleucines, 6 valines, and 5 alanines. In the VIA-(i + 1)–HSQC (a) all expected signals of Val/Ile neighbors appear (only five Ile (i + 1) can appear since Ile-4 has a proline as a sequential neighbor). In the VIA-(i, i + 1)–HSQC (b) all signals from Val and Ile are visible. Thr signals are well suppressed in both experiments. Alanine signals are marked with thin rectangles. The Ala signals can be identified easily using the A-(i + 1) and A-(i, i + 1) experiments (*37*). (c) The LA-(i + 1)–HSQC was acquired in 2 h 15 min using 48 scans per complex point. (d) The LA-(i, i + 1)–HSQC was acquired in 4 h 30 min using 96 scans per complex point. The SAM domain contains 5 leucines. In the LA-(i + 1)–HSQC (c) signals from sequential neighbors of 4 Leu are present together with the sequential neighbors of Ala (marked with rectangles); D18 (L17) is absent. Since the suppression of Val/Ile/Thr is only based on appropriate tuning of T_R together with selective pulses, the suppression is not perfect. Weak negative or positive signals of Val/Ile/Thr could appear (marked with *). In the LA-(i, i + 1)–HSQC (d) four Leu signals are visible; L17 is absent. All signals of Ala-residues (marked with thin rectangles) and their sequential neighbors are present. The (i + 1) peaks are marked with thick rectangles. They can be identified by comparison with the LA-(i + 1)–HSQC. Again the suppression of Thr/Ala/Val is not perfect and the signal of T3 is visible.

The Thr-C^{β} is not affected by any of the three selective pulses. The magnetization C_x^{γ} can therefore not evolve into antiphase magnetization with respect to the C^{β} during $2\tau_1'$ and $2T_R'$. During $2T_R$ the antiphase magnetization $2C_y^{\gamma}C_z^{\beta}$ is created and converted into $2C_z^{\gamma}C_y^{\beta}$ by the next 90° pulse. This antiphase magnetization is not refocused during T_C (or δ_3). No magnetization is therefore transferred to C^{α} and Thr is suppressed. From similar consideration it is clear that signals from Ala will not be suppressed.

Starting from the γ-CH_3 of Val and Ile there are three possible magnetization pathways. There are three relay steps in the beginning of pulse sequence while it takes only two steps

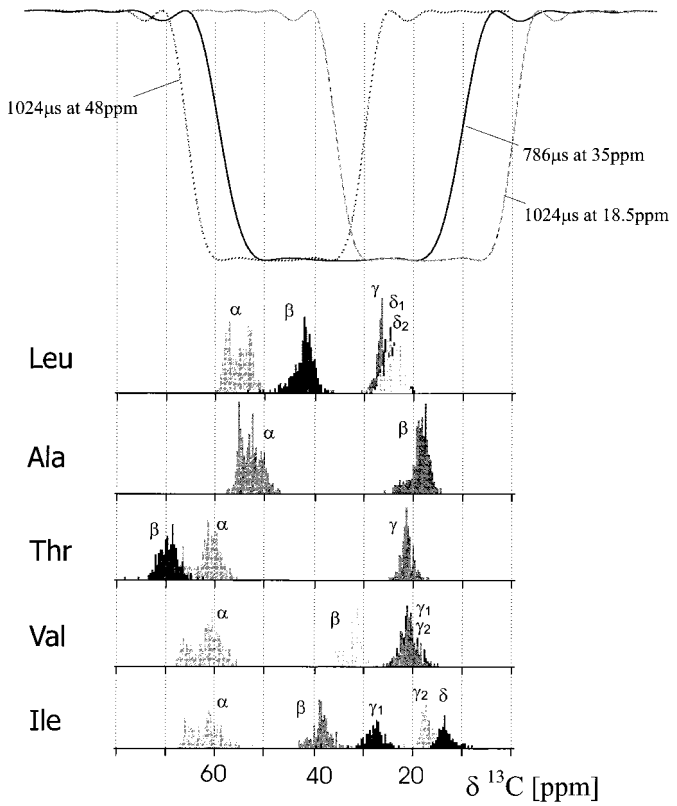

FIG. 6. For the LA–HSQCs three pulses with a REBURP profile are used. The pulses S_1, S_2, and S_3 (Figs. 2e and 2f) have a length of 1024, 768, and 1024 μs and are centered at 18.5, 35, and 48 ppm, respectively. The simulated inversion profiles (for 600-MHz ^{1}H frequency) of the selective pulses are shown at the top. The inversion profiles were simulated with the shape tool of XWINNMR2.6. The refocusing profiles show similar plateaus in the same range. At the bottom statistical ^{13}C chemical shift data from the BioMagResBank database (*46*) are given for Leu, Ala, Thr, Val, and Ile (reproduced with kind permission from BMRB).

to transfer the magnetization from the C^γ to the C^α. Consequently, the magnetization may stay in-phase during any of the steps and still result in a detectable signal. Depending on the delay during which no antiphase magnetization is created, this results in the three possible transfer functions for the $(i + 1)$ sequence:

$$\cos(\pi J_{CC}2\tau_1')\sin(\pi J_{CC}2T_R') \times \sin^2(\pi J_{CC}2T_R)\cos(\pi J_{CC}2T_R)\sin(\pi J_{CC}2T_C) \quad [8]$$

$$\sin(\pi J_{CC}2\tau_1')\sin(\pi J_{CC}2T_R') \times \cos^2(\pi J_{CC}2T_R')\sin(\pi J_{CC}2T_R)\sin(\pi J_{CC}2T_C) \quad [9]$$

$$\sin(\pi J_{CC}2\tau_1')\sin^2(\pi J_{CC}2T_R') \times \cos(\pi J_{CC}2T_R')\sin(\pi J_{CC}2T_R)\cos(\pi J_{CC}2T_C). \quad [10]$$

The transfer functions for the $(i, i + 1)$ experiment are identical, except that T_C is replaced by δ_3. If no selective pulses are used, all three pathways lead to detectable magnetization. The selective pulse S_1 refocuses the coupling between Ile-C^β and $C^{\gamma 2}$ and partially also between Val-C^β and C^γ during $2\tau_1'$ so that the last two pathways [9] and [10] are almost completely suppressed. While $T_R = 1/2J_{CC}$ (14.2 ms) is optimal for Leu, the first pathway [8] for Ile/Val is suppressed because $\cos(\pi J_{CC}2T_R)$ becomes zero. The reason is that C^β magnetization of Val and Ile evolves into antiphase magnetization with respect to the second C^γ during T_R and the next 90° pulse converts it into multiple-quantum coherence that is not converted back into detectable magnetization during the rest of the pulse sequence.

Starting from the δ-CH_3 of Ile magnetization can also be transferred to the C^α. This pathway is suppressed in the same manner described for magnetization starting from the C^γ of Val and Ile by setting $T_R = 1/2J_{CC}$. During this delay magnetization originating form the C^δ of Ile has reached the C^β. Antiphase magnetization with respect to the C^α and the second C^γ of Ile is created and subsequently converted into undetectable multiple-quantum coherence.

Because of the variation of J_{CC} between the side chain carbons of Val, Ile, and Thr the suppression of the signals from those amino acids will not be perfect. The corresponding spectra are shown in Figs. 5c and 5d.

CONCLUSION

We have presented a set of new pulse sequences that yield amino acid type-selective ^{1}H–^{15}N correlations. Together with the recently published selective ^{1}H–^{15}N correlations, we now have a set of 22 experiments which allow us to identify the ^{1}H–^{15}N resonances of Gly, Ala, Thr, Ile/Val, Asn, Gln, Ser, Leu, Asp, and Glu residues and their sequential neighbors in a ^{15}N-HSQC spectrum. Some of the pulse sequences yield spectra that contain signals of only one type of amino acid (G, A, S, N). The other amino acids can then be identified from combinations of these spectra with others containing more than one type of amino acid: Thr from A and TA spectra, Val and Ile from A and VIA spectra, Leu from A and LA spectra, Q from N and NQ spectra, D from G, N, and DNG spectra, and finally E from N, NQ, G, and EQG spectra. The signals from Val and Ile cannot be distinguished, although the signals from Val tend to be stronger since two CH_3 groups contribute to the resulting peak.

The implementation of MUSIC into triple-resonance experiments does not lengthen the sequence, therefore no loss of intensity due to relaxation is observed. While the CH_3 selection reduced the intensity of the peaks by 25%, no reduction occurs with the CH_2 selection. Consequently, the sensitivity of the selective experiments is comparable to that of the standard triple-resonance experiments from which the new sequences have been derived: The sequences transferring the magnetization to the amide proton via the C^α exhibit lower sensitivity

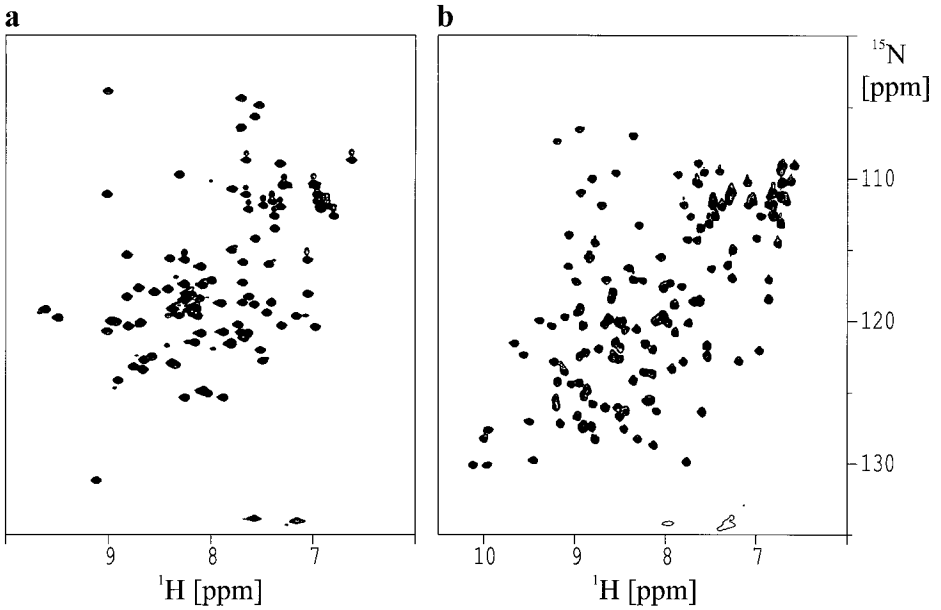

FIG. 7. ^{15}N-HSQC of the two protein domains used for the new experiments. The spectra are given as a comparison for the spectra from the new selective experiments (Figs. 3–5). (a) HSQC of the SAM domain from EphB2 (*40, 41*), a protein of 83 residues, (b) HSQC of the EVH1 domain from VASP (*42, 43*), a protein of 115 residues.

than those that transfer via the carbonyl carbon; the sequences with multiple relay steps are less sensitive than those with just one transfer-step. The most sensitive experiment is therefore the G–(i + 1)-HSQC while the LA- and the NQ–(i, i + 1)-HSQC are the least sensitive experiments. When the proteins become too large for standard triple-resonance, the selective experiments will fail as well. Most of the sequences will not work with deuterated proteins, since the selection with MUSIC assumes fully protonated side chains. Exceptions are the N and the NQ experiments that select for NH_2 groups. We also applied the LA– and the VIA–HSQCs to a protein sample with methyl protonation (*52, 53*). Here the sequences work well (data not shown) and can provide useful information.

The two-dimensional spectra presented here may be used in addition to the conventional three-dimensional spectra to aid either manual or automated assignment. These spectra take only a small amount of spectrometer time and provide valuable additional information. A problem accompanying the use of these experiments in automated assignment procedures is the presence of spurious signals from nonselected residues. The type of amino acid that will give rise to breakthrough peaks is known beforehand, however, and they can be identified from comparison with other spectra. Breakthrough peaks of Asn/Asp in the EQG spectra can be identified with the DNG spectra and breakthrough peaks of Val/Ile/Thr in the LA experiments with the VIA and TA spectra. Different combinations of spectra will be evaluated with our automated assignment program catch23 (*7*) and results will be presented elsewhere.

EXPERIMENTAL

The spectra were recorded on a DRX600 in standard configuration using an inverse triple-resonance probe equipped with three-axis self-shielded gradient coils. Two different protein domains were used for the experiments. The DNG and EQG experiments were recorded with a 1.35 mM sample of the EVH1 domain from VASP uniformly labeled with ^{15}N and ^{13}C. For all other experiments a 1.5 mM sample of the SAM domain from EphB2 (PDB: 1SGG) uniformly labeled with ^{15}N and ^{13}C was used. For both samples 5-mm ultraprecision sample tubes were used. The HSQC spectra of both domains are shown in Fig. 7 as a comparison for the spectra shown in Figs. 3, 4, and 5. The HSQC of the SAM domain (Fig. 7a) was recorded with 512 complex points in each dimension, a spectral width of 3012 Hz (^{15}N) × 10,000 Hz (^{1}H), and 8 transients. All other spectra were recorded in an identical way but with 64 (t_1) × 512 (t_2) complex points. The data were processed using a squared sinebell shifted by 90° as a window function in both dimensions. The ^{15}N t_1 interferograms were quadrupled in length by linear prediction using XWINNMR, except for the spectrum of the SAM domain. The final spectra had a size of 512 (t_1) × 1024 (t_2) real points. The pulse programs and the L0S2-0 shape in Bruker format are available upon request.

ACKNOWLEDGMENTS

Support from the Forschungsinstitut für Molekulare Pharmakologie is gratefully acknowledged. Mario Schubert is supported by the DFG Graduiertenkol-

leg GRK 80 "Modellstudien." The authors thank Linda Ball for the assignment of the EVH1 domain, Thomas Jarchau for the preparation of the EVH1 sample, Maika Smalla for the preparation and the assignment of the SAM-domain, and Wolfgang Bermel and Rüdiger Winter for helpful discussions. The work was supported by a grant of the BMBF (01 GG 9812, Leitprojekt "Proteinstrukturfabrik").

REFERENCES

1. G. T. Montelione and G. Wagner, Conformation-independent sequential NMR connections in isotope-enriched polypeptides by ^{1}H–^{13}C–^{15}N triple-resonance experiments, *J. Magn. Reson.* **87,** 183–188 (1990).
2. L. E. Kay, M. Ikura, R. Tschudin, and A. Bax, Three-dimensional triple-resonance NMR spectroscopy of isotopically enriched proteins, *J. Magn. Reson.* **89,** 496–514 (1990).
3. D. E. Zimmerman and G. T. Montelione, Automated analysis of nuclear magnetic resonance assignments for proteins, *Curr. Opin. Struct. Biol.* **5,** 664–673 (1995) and references cited therein.
4. K. B. Li and B. C. Sanctuary, Automated resonance assignment of proteins using heteronuclear 3D NMR. 1. Backbone spin systems extraction and creation of polypeptides, *J. Chem. Inf. Comput. Sci.* **37,** 359–366 (1997).
5. K. B. Li and B. C. Sanctuary, Automated resonance assignment of proteins using heteronuclear 3D NMR. 2. Side chain and sequence-specific assignment, *J. Chem. Inf. Comput. Sci.* **37,** 467–477 (1997).
6. D. E. Zimmerman, C. A. Kulikowski, Y. Huang, W. Feng, M. Tashiro, S. Shimotakahara, Ch. Chien, R. Powers, and G. T. Montelione, Automated analysis of protein NMR assignments using methods from artificial intelligence, *J. Mol. Biol.* **269,** 592–610 (1997).
7. D. Croft, J. Kemmink, K.-P. Neidig, and H. Oschkinat, Tools for the automated assignment of high-resolution three-dimensional protein NMR spectra based on pattern recognition techniques, *J. Biomol. NMR* **10,** 207 (1997).
8. M. Leutner, R. M. Gschwind, J. Liermann, C. Schwarz, G. Gemmecker, and H. Kessler, Automated backbone assignment of labeled proteins using the threshold accepting algorithm, *J. Biomol. NMR* **11,** 31–43 (1998).
9. M. Sattler, J. Schleucher, and C. Griesinger, Heteronuclear multidimensional NMR experiments for the structure determination of proteins in solution employing pulsed field gradients, *Prog. NMR Spectrosc.* **34,** 93–158 (1999).
10. J. Cavanagh, W. J. Fairbrother, A. G. Palmer III, and N. J. Skelton, "Protein NMR Spectroscopy," Academic Press, San Diego, 1996.
11. G. M. Clore and A. M. Gronenborn, Application of three- and four-dimensional heteronuclear NMR spectroscopy to protein structure determination, *Prog. NMR Spectrosc.* **23,** 43–92 (1991).
12. R. T. Clowes, A. Crawford, A. R. C. Raine, B. O. Smith, and E. D. Laue, Improved methods for structural studies of proteins using nuclear magnetic resonance spectroscopy, *Curr. Opin. Struct. Biol.* **6,** 81–88 (1995).
13. H. N. Moseley and G. T. Montelione, Automated analysis of NMR assignments and structures for proteins, *Curr. Opin. Struct. Biol.* **9,** 635–642 (1999) and references cited therein.
14. G. T. Montelione, C. B. Rios, G. V. T. Swapna, and D. E. Zimmerman, NMR pulse sequences and computational approaches for automated analysis of sequence-specific backbone resonance assignments of proteins, *Biol. Magn. Reson.* **17,** 81–130 (1999).
15. S. Grzesiek and A. Bax, Amino acid type determination in the sequential assignment procedure of uniformly $^{13}C/^{15}N$-enriched proteins, *J. Biomol. NMR* **3,** 185–204 (1993).
16. N. S. Rao, P. Legault, D. R. Muhandiram, J. Greenblatt, J. L. Battiste, J. R. Williamson, and L. E. Kay, NMR pulse schemes for the sequential assignment of arginine side-chain H^{ϵ} protons, *J. Magn. Reson. B* **113,** 272–276 (1996).
17. H. Vis, R. Boelens, M. Mariani, R. Stroop, C. E. Vorgias, K. S. Wilson, and R. Kaptein, ^{1}H, ^{13}C, and ^{15}N resonance assignments and secondary structure analysis of the HU protein from Bacillus stearothermophilus using two- and three-dimensional double- and triple-resonance heteronuclear magnetic resonance spectroscopy, *Biochemistry* **33,** 14858–14870 (1994).
18. T. Yamazaki, S. M. Pascal, A. U. Singer, J. D. Forman-Kay, and L. E. Kay, NMR pulse schemes for the sequence-specific assignment of arginine guanidino ^{15}N and ^{1}H chemical shifts in proteins, *J. Am. Chem. Soc.* **117,** 3556–3564 (1995).
19. M. Pellecchia, G. Wider, H. Iwai, and K. Wüthrich, Arginine side chain assignments in uniformly ^{15}N-labeled proteins using the novel 2D HE(NE)HGHH experiment, *J. Biomol. NMR* **10,** 193–197 (1997).
20. C. Zwahlen, S. J. F. Vincent, K. H. Gardner, and L. E. Kay, Significantly improved resolution for NOE correlations from valine and isoleucine ($C^{\gamma 2}$) methyl groups in ^{15}N,^{13}C- and ^{15}N, ^{13}C, ^{2}H-labeled proteins, *J. Am. Chem. Soc.* **120,** 4825–4831 (1998).
21. M. Wittekind, W. J. Metzler, and L. Mueller, Selective correlations of amide groups to glycine alpha protons in proteins, *J. Magn. Reson. B* **101,** 214–217 (1993).
22. E. T. Olejniczak and S. W. Fesik, Two-dimensional nuclear magnetic resonance method for identifying the H^{α}/C^{α} signals of amino acid residues preceding proline, *J. Am. Chem. Soc.* **116,** 2215–2216 (1994).
23. K. Gehring and E. Guittet, Two-dimensional nuclear magnetic resonance method for identifying the H_N/N signals of amino-acid residues following glycine, *J. Magn. Reson. B* **109,** 206–208 (1995).
24. M. Tashiro, C. B. Rios, and G. T. Montelione, Classification of amino acid spin systems using PFG HCC(CO)NH-TOCSY with constant-time aliphatic ^{13}C frequency labeling, *J. Biomol. NMR* **6,** 211–216 (1995).
25. B. T. Farmer II and R. A. Venters, Assignment of aliphatic side-chain $^{1}H/^{15}N$ resonances in perdeuterated proteins, *J. Biomol. NMR* **7,** 59–71 (1996).
26. W. Feng, C. B. Rios, and G. T. Montelione, Phase labeling of C–H and C–C spin-system topologies: Application in PFG-HACANH and PFG-HACA(CO)NH triple-resonance experiments for determining backbone resonance assignments in proteins, *J. Biomol. NMR* **8,** 98–104 (1996).
27. C. B. Rios, W. Feng, M. Tashiro, Z. Shang, and G. T. Montelione, Phase labeling of C–H and C–C spin-system topologies: Application in constant-time PFG-CBCA(CO)NH experiments for discriminating amino acid spin-system types, *J. Biomol. NMR* **8,** 345–350 (1996).
28. V. Dötsch, R. E. Oswald, and G. Wagner, Amino-acid-type-selective triple-resonance experiments, *J. Magn. Reson. B* **110,** 107–111 (1996).
29. V. Dötsch, R. E. Oswald, and G. Wagner, Selective identification of threonine, valine, and isoleucine sequential connectivities with a TVI-CBCACONH experiment, *J. Magn. Reson. B* **110,** 304–308 (1996).
30. V. Dötsch and G. Wagner, Editing for amino-acid type in CBCACONH experiments based on the $^{13}C^{\beta}$–$^{13}C^{\gamma}$ coupling, *J. Magn. Reson. B* **111,** 310–313 (1996).

31. V. Dötsch, H. Matsuo, and G. Wagner, Amino-acid-type identification for deuterated proteins with a β-carbon-edited HNCOCACB experiment, *J. Magn. Reson. B* **112,** 95–100 (1996).
32. F. Löhr and H. Rütherjans, H_2NCO-E.COSY, a simple method for the stereospecific assignment of side-chain amide protons in proteins, *J. Magn. Reson.* **124,** 255–258 (1997).
33. M. Pellecchia, H. Iwai, T. Szyperski, and K. Wüthrich, The 2D NMR experiments H(C)CO_2 and H$\underline{CCO}_2$ for assignment and pH titration of carboxylate groups in uniformly ^{15}N/^{13}C-labeled proteins, *J. Magn. Reson.* **124,** 274–278 (1997).
34. D. R. Muhandiram, P. E. Johnson, D. Yang, O. Zhang, L. P. McIntosh, and L. E. Kay, Specific ^{15}N, NH correlations for residues in ^{15}N, ^{13}C and fractionally deuterated proteins that immediately follow methyl-containing amino acids, *J. Biomol. NMR* **10,** 283–288 (1997).
35. R. Bazzo, D. O. Cicero, and G. Barbato, Selective correlation of amide groups to glycine alpha protons and of arginine guanidine groups to delta protons in proteins by multiple quantum spectroscopy, *J. Magn. Reson.* **136,** 15–21 (1999).
36. M. J. Bottomley, M. J. Macias, Z. Liu, and M. Sattler, A novel NMR experiment for the sequential assignment of proline residues and proline stretches in ^{13}C/^{15}N-labeled proteins, *J. Biomol. NMR* **13,** 381–385 (1999).
37. M. Schubert, M. Smalla, P. Schmieder, and H. Oschkinat, MUSIC in triple-resonance experiments: Amino acid type-selective ^{1}H–^{15}N correlations, *J. Magn. Reson.* **141,** 34–43 (1999).
38. P. Schmieder, M. Leidert, M. Kelly, and H. Oschkinat, Multiplicity-selective coherence transfer steps for the design of amino acid-selective experiments—A triple-resonance experiment selective for Asn and Gln, *J. Magn. Reson.* **131,** 199–202 (1998).
39. P. Schmieder, M. Smalla, and H. Oschkinat, New amino-acid selective NMR experiments for the assignment of Asn and Gln in proteins, *in* "Proceedings of the 29. AMPERE-13. ISMAR International Conference on Magnetic Resonance and Related Phenomena" (D. Ziessow and W. Lubitz, Eds.), pp. 134–135, Berlin, 1998.
40. C. P. Ponting, SAM: A novel motif in yeast sterile and Drosophila polyhomeotic proteins, *Protein Sci.* **4,** 1928–1930 (1995).
41. M. Smalla, P. Schmieder, M. Kelly, A. ter Laak, G. Krause, L. Ball, M. Wahl, P. Bork, and H. Oschkinat, Solution structure of receptor tyrosine kinase EphB2 SAM domain and identification of two distinct homotypic interaction sites, *Protein Sci.* **8,** 1954–1961 (1999).
42. I. Callabaut, P. Crossart, and P. Dehoux, EVH1/Whether domains of VASP and WASP proteins belong to a large family including Ran-binding domains of RanBP1 family, *FEBS Lett.* **441,** 181–185 (1999).
43. L. J. Ball, R. Kühne, B. Hoffmann, A. Häfner, P. Schmieder, R. Volkmer-Engert, M. Hof, M. Wahl, J. Schneider-Mergenes, U. Walter, H. Oschkinat, and T. Jarchau. Dual epitope recognition by the VASP EVM1 domain modulates polyproline ligand specificity and binding affinity, *EMBO J.* **19,** 4903–4914 (2000).
44. S. Grzesiek and A. Bax, Correlating backbone amide and side chain resonances in larger proteins by multiple relayed triple resonance NMR, *J. Am. Chem. Soc.* **114,** 6291–6293 (1992).
45. S. Grzesiek and A. Bax, An efficient experiment for sequential backbone assignment of medium-sized isotopically enriched proteins, *J. Magn. Reson. B* **99,** 201–207 (1992).
46. http://www.bmrb.wisc.edu.
47. H. Geen and R. Freeman, Band-selective radiofrequency pulses, *J. Magn. Reson.* **93,** 93–141 (1991).
48. L. Müller, Sensitivity enhanced detection of weak nuclei using heteronuclear multiple quantum coherence, *J. Am. Chem. Soc.* **101,** 4481–4484 (1979).
49. A. Bax, R. H. Griffey, and B. L. Hawkins, Correlation of proton and nitrogen-15 chemical shifts by multiple quantum NMR, *J. Magn. Reson.* **55,** 301–315 (1983).
50. E. Lunati, P. Cofrancesco, M. Villa, P. Marzola, and F. Osculati, Evolution strategy optimization for selective pulses in NMR, *J. Magn. Reson.* **134,** 223–235 (1998).
51. http://matsci.unipv.it/persons/lunati/pulses.htm.
52. M. K. Rosen, K. H. Gradener, R. C. Willis, W. E. Parris, T. Pawson, and L. E. Kay, Selective methyl group protonation of perdeuterated proteins, *J. Mol. Biol.* **263,** 627–636 (1996).
53. K. H. Gardener, R. Konrat, M. K. Rosen, and L. E. Kay, An (H)C(CO)NH–TOCSY pulse scheme for sequential assignment of protonated methyl groups in otherwise deuterated ^{15}N,^{13}C-labeled proteins, *J. Biomol. NMR* **8,** 351–356 (1996).
54. L. Emsley and G. Bodenhausen, Gaussian pulse cascades: New analytical functions for rectangular selective inversion and in-phase excitation in NMR, *Chem. Phys. Lett.* **165,** 469–476 (1990).
55. A. J. Shaka, J. Keeler, T. Frenkiel, and R. Freeman, An improved sequence for broadband decoupling: WALTZ-16, *J. Magn. Reson.* **52,** 335–338 (1983).
56. A. J. Shaka, P. B. Barker, and R. Freeman, Computer-optimized decoupling scheme for wideband applications and low-level operation, *J. Magn. Reson.* **64,** 547–552 (1985).
57. V. Sklenar, M. Piotto, R. Leppik, and V. Saudek, Gradient-tailored water suppression for ^{1}H–^{15}N HSQC experiments optimized to retain full sensitivity, *J. Magn. Reson. A* **102,** 241–245 (1993).
58. D. Marion, M. Ikura, R. Tschudin, and A. Bax, Rapid recording of 2D NMR spectra without phase cycling, application to the study of hydrogen exchange, *J. Magn. Reson.* **85,** 393–399 (1989).